

Update on Chiral Symmetry Restoration in the Context of Dilepton Data

Ralf Rapp

Cyclotron Institute and Department of Physics and Astronomy, Texas A&M University,
College Station, TX 77843-3366, U.S.A.

E-mail: rapp@comp.tamu.edu

Abstract. We evaluate currently available information on low-mass dilepton and direct-photon emission spectra measured in ultrarelativistic heavy-ion collisions. In the first part an attempt is made to develop a consistent picture of the in-medium effects on the electromagnetic spectral function and pinpoint its emission history by utilizing its radial and elliptic flow signatures. In the second part we elaborate on the implications of the empirical information on the nature of chiral symmetry restoration. We indicate how the melting of the ρ resonance in hot and dense matter is related to, and compatible with, the reduction of chiral order parameters as “measured” in thermal lattice QCD.

1. Introduction

The spontaneous breaking of chiral symmetry (SBCS) in the QCD vacuum is believed to be a consequence of the condensation of scalar quark-antiquark pairs. It manifests itself in the generation of mass in strong interactions and, more precisely, in lifting the degeneracies within chiral multiplets (π - σ , ρ - a_1 , N - $N^*(1535)$, ...). The search for (partial) restoration of SBCS in hot and dense matter as a fundamental phenomenon is one of the core missions of the ultrarelativistic heavy-ion programs at laboratories around the world. The most promising observable in this regard are invariant-mass spectra of dileptons (e^+e^- or $\mu^+\mu^-$) which open a direct window on the in-medium spectral function of the electromagnetic (EM) current, cf. Refs. [1, 2, 3, 4, 5] for recent reviews. In the vacuum, and at low mass ($M \leq 1$ GeV), the EM spectral function reflects the mass distribution of the light vector mesons ρ , ω and ϕ , and thus the dynamical generation of mass in QCD. Thermal radiation of low-mass dileptons is ideally suited to illuminate the changes in the vector-meson mass distributions as the (pseudo-) critical temperature for chiral restoration, $T_{pc}^X \simeq 160$ MeV, is approached and surpassed. However, robust conclusions from measurements of dilepton spectra in heavy-ion collisions require a number of rather challenging steps. First, one needs sufficiently accurate measurements of so-called “excess” radiation (beyond final-state decays) to extract its spectral shape. Second, such measurements need to cover a large range of collision energies to establish systematic trends, enabling the extraction of genuine features in the radiation. In particular, one needs to correlate the observed spectral shapes with the thermodynamic properties of the emission sources, most notably its temperature(s). Third, model calculations and predictions need to be tested against the data which is critical for deducing mechanisms underlying observed spectral modifications. Such comparisons not only require calculations of the in-medium EM spectral functions but also a good control over space-

time evolution of the fireball at each collision energy. Finally, the model calculations have to be rooted in the bigger picture of QCD thermodynamics, and specifically in the context of chiral restoration by utilizing relations between the EM spectral functions and chiral order parameters, where the latter can be tested (or extracted) from thermal lattice QCD. It is the purpose of this proceedings to give an update on carrying out these steps.

The remainder of this article is organized into two main sections. The first one (Sec. 2) contains a phenomenological assessment of the current experimental situation regarding the extraction of the in-medium EM spectral function and the pertinent regimes in temperature and baryon density that it corresponds to. The second one (Sec. 3) summarizes how the phenomenological findings relate to chiral symmetry restoration, invoking both rigorous and more heuristic arguments. Both sections are not divided up any further to stipulate the comprehensive nature of the discussion. We briefly conclude in Sec. 4.

2. Electromagnetic Emission Spectra from Experiment

The first unambiguous detection of a low-mass dilepton excess in ultrarelativistic heavy-ion collisions (URHICs) was achieved by the CERES/NA45 collaboration, first in the S-Au system [6] and later with improved precision in Pb-Au collisions [7, 8]. Early theoretical analyses successfully described these data utilizing the conjecture of a dropping ρ -meson mass in hot and dense matter [9], as a direct consequence of the reduction of the quark condensate (later, this connection was found to be problematic and revisited [10]). Shortly thereafter, several groups started to evaluate “more mundane” medium modifications, by performing “standard” hadronic many-body (or thermal-field theory) calculations of the ρ spectral function using *known* (or at least well-constrained) hadronic interactions in vacuum as an input. These calculations, performed for cold nuclear matter [11, 12, 13, 14, 15, 16, 17], a hot meson gas [18, 19, 20, 21, 22], or hot and dense hadronic matter [23, 24, 25, 26], generically produce a rather strong broadening of the in-medium ρ spectral function with little mass shift, especially in nuclear media. What was originally intended to provide a baseline for disentangling more “exotic” medium effects, subsequently turned into a fair description of the CERES dilepton enhancement all by itself, see the left panel of Fig. 1. Does this imply that dilepton data are not sensitive (or even unrelated) to chiral restoration? Our answer is no, as will be discussed in Sec. 3 below.

A quantitative test of the “ ρ -broadening” became possible with the NA60 dimuon spectra in In-In($\sqrt{s}=17.3$ AGeV) collisions [29, 27], which have set a new standard for precision in dilepton spectroscopy in URHICs to date, see right panel of Fig. 1. These data have been fully corrected for the detector acceptance, which, for the first time in URHIC dilepton spectroscopy, renders the mass spectra (Lorentz-) *invariant*. This means that their shape is *unaffected* by the blue shift due to the collective flow of the expanding fireball, and thus they directly reflect the spectral distribution of the medium’s emission rate (in addition, the excellent mass resolution and statistics allowed for a subtraction of the hadronic decay cocktail, defining the notion of “excess” spectra). If the emission emanates from a locally thermalized medium, it takes the well-known form

$$\frac{dN_{ll}}{d^4x d^4q} = -\frac{\alpha_{\text{em}}^2}{\pi^3 M^2} f^B(q_0; T) \text{Im}\Pi_{\text{em}}(M, q; \mu_B, T), \quad (1)$$

where $\text{Im}\Pi_{\text{em}}$ is the in-medium EM spectral function, f^B the thermal Bose distribution and the factor $1/M^2$ is a remnant of the intermediate propagator of the virtual photon. The predictions of hadronic many-body theory (evolved over a thermal fireball evolution constrained by hadron spectra) [30, 28] turn out to agree well with these data, cf. right panel of Fig. 1 (see also Refs. [31, 32, 33, 34]). This actually provides non-trivial information beyond the realm of strict reliability of hadronic theory, which we estimate to be up to $T \simeq 150$ MeV, where the total hadron density reaches about $2\rho_0$ ($\rho_0=0.16$ fm $^{-3}$ denotes nuclear matter saturation density). A good portion of the low-mass dilepton enhancement is radiated from temperatures around and

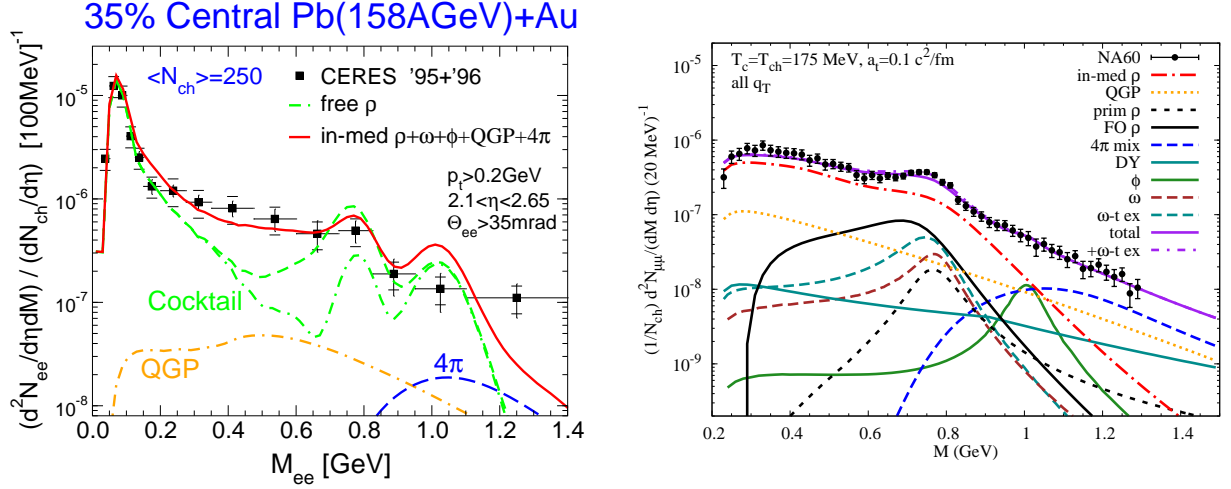


Figure 1. Dilepton spectra measured at SPS energies ($\sqrt{s}=17.3$ AGeV) by the CERES/NA45 collaboration in Pb-Au collisions (left panel) [7], and by the NA60 collaboration in In-In (right panel) [27], compared to the same theoretical approach [28]. The CERES data are taken in the e^+e^- channel and include acceptance cuts in the (di-) electron tracks, while the NA60 data are for $\mu^+\mu^-$, subtracted of the cocktail and fully corrected for (di-) muon acceptance cuts.

somewhat below T_{pc} in the fireball evolution. In other words, the NA60 data quantitatively support a smooth extrapolation of the hadronic ρ broadening into the temperature region of the chiral transition. More explicitly, the observed spectra follow from a convolution of the above rate, Eq. (1), over 3-momentum and 4-volume of the expanding medium,

$$\frac{dN_{ll}}{dM dy} = \frac{1}{\Delta y} \int_{\tau_0}^{\tau_{fo}} d\tau \int_{V_{FB}} d^3x \int \frac{M d^3q}{q_0} \frac{dN_{ll}}{d^4x d^4q}(M, q; T(\tau), \mu_B(\tau)) \quad (2)$$

$$\simeq \frac{V_4}{\Delta y} \int \frac{d^3q}{M q_0} \frac{\alpha_{em}^2}{\pi^3} f^B(q_0; \bar{T}) (-\text{Im}\Pi_{em}(M, q; \bar{T}, \bar{\mu}_B)) . \quad (3)$$

In the second line we have condensed the space-time integration into a 4-volume, V_4 , at the expense of replacing the time-dependent temperature and baryo-chemical potential (or baryon density) in the dilepton rate by average values, \bar{T} and $\bar{\mu}_B$, respectively. The latter can be extracted from the model calculations which describe the data to be $\bar{T} \simeq 150$ -160 MeV and $\bar{\mu}_B^{\text{tot}} \simeq 250$ -300 MeV (or $\bar{\rho}_B^{\text{tot}} \simeq 0.7$ -1 ρ_0). The remaining 3-momentum integral in Eq. (3) is a Lorentz scalar and can thus be evaluated in the local rest frame. This is routinely done in model calculations of the spectral function, as shown in the left panel of Fig. 2, including the dimuon phase-space factor and mass threshold, $M_{\text{thr}} = 2m_\mu = 211$ MeV. One immediately recognizes a remarkable reminiscence of the theoretical rates, calculated a decade ago [24], with the NA60 data. This corroborates the possibility of extracting an “average” ρ -meson width which turns out to be $\bar{\Gamma}_\rho^{\text{med}} \simeq 350$ -400 MeV (which is not far from the value found for cold nuclear matter at saturation density). This necessarily implies larger widths in the earlier stages of the fireball evolution (later and earlier contributions are, in fact, required to properly account for the total excess yield), which reach around $\Gamma_\rho(T_{pc}) \simeq 600$ MeV, before a transition to QGP rates is performed. At this point, the QGP and hadronic rates are very similar (see left panel of Fig. 2), which has been interpreted as quark-hadron duality in dilepton rates across T_{pc} [35]. A similar feature was found for photon rates in Ref. [36], and later again in Ref. [37].

An important question is whether one can obtain independent information on the medium’s

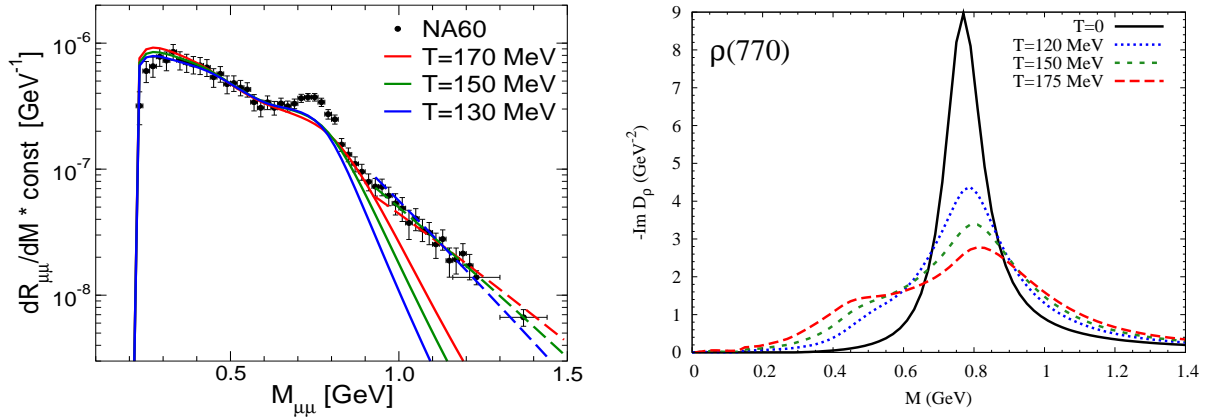


Figure 2. Left panel: Comparison of the thermal dilepton emission rates at fixed temperature (as figuring into the full calculation of the spectra shown in Fig. 1) with the acceptance corrected NA60 spectra. The rates are a combination of the low-mass ρ contribution (solid lines) and a continuum “ 4π ” part (dashed lines) which for simplicity has been approximated by a perturbative continuum limited to $M > 0.9$ GeV. Both contributions carry the relative normalization as used in the fireball evolution (including pion fugacity factors), but are scaled by an overall constant to match the data at $M \simeq 0.5$ GeV. Isoscalar contributions (ω and ϕ) to the rates are not included. Right panel: In-medium ρ spectral function based on Ref. [24] as figuring into the calculations of the dilepton spectra in Fig. 1 [28] and underlying the low-mass in-medium hadronic rates in the left panel.

temperature from which the observed spectral shape is originating. As stated above, invariant-mass spectra are an ideal tool to evaluate emission temperatures due to the absence of blue shifts induced by the collective flow (which are present in transverse-momentum (q_T) spectra). However, as evident from Eq. (3), the thermal slope associated with the Bose distribution is modulated by the medium effects in the EM spectral function. Nevertheless, when using the in-medium hadronic rates underlying the description of the NA60 data in Fig. 1 (right) as a “thermometer”, one finds that the slope in the data over the range $M = 0.3$ - 1.5 GeV is reasonably well reproduced with $T \simeq 150$ - 170 MeV, cf. left panel of Fig. 2. Closer inspection of this comparison reveals that the enhancement at the very low-mass end, close to the dimuon threshold, is slightly overestimated, suggesting that in this regime emission from later stages prevails, where the medium effects are smaller, cf. the in-medium ρ spectral function in the right panel of Fig. 2. Alternatively, carrying out the slope analysis for masses above $M = 1$ GeV, where the medium effects on the rate are less pronounced (resembling a structureless continuum), one deduces a slope of around $T \simeq 170$ MeV up to $M \simeq 1.5$ GeV, with a tendency to further increase at still higher mass. This is consistent with the well-known feature that at higher mass (or higher q_T , as governed by the energy, q_0 , figuring into the thermal distribution function), the temperature sensitivity of the thermal exponential increasingly biases the contributions to the spectra toward earlier phases (i.e., higher T) [4]. The NA60 collaboration has also conducted a systematic investigation of slope parameters, T_{eff} , of q_T spectra in various mass bins [38]. Here, T_{eff} contains the radial-flow blue shift, schematically as $T_{\text{eff}} \simeq T + M\beta_{\text{av}}^2$, where β_{av} denotes the average expansion velocity of the fireball at a given moment. The extracted values for T_{eff} gradually increase from about 170 MeV at threshold up to ca. 260 MeV at the ρ mass, decreasing thereafter and leveling off at ca. 200-220 MeV for $M > 1$ GeV. This is remarkably consistent

with the information from M -spectra, i.e., an emission source of hot hadronic matter at and below the ρ -mass with a mass-dependent slope increase, and emission from around T_c and higher (with a possibly large QGP component) above the ρ mass.

An intriguing aspect of the ρ -broadening as obtained from many-body theory in hot and dense hadronic matter is the prevalence of baryon-induced medium effects [23, 24]. Theoretically, this is a consequence of quantitative constraints on the ρ -meson coupling to nucleons as deduced, e.g., from nuclear photoabsorption data on the proton and on nuclei [39]. This feature raised some doubts in the early stages of interpreting the CERES data, as the experimental pion-to-baryon ratio at full SPS energy is about 5:1. However, many of the pions observed in the final state originate from resonance decays; including these in a thermally equilibrated “hadron resonance gas” gives meson-to-baryon ratios of closer to 2:1. Nonetheless, the question arises how the properties of the excess radiation develop with the nuclear collision energy, i.e., with the relative baryon content in the system. The first step in this direction was a CERES measurement at a lower SPS bombarding energy of $E_{\text{lab}}=40$ AGeV ($\sqrt{s}=8.7$ AGeV) [40]. While the pion multiplicity decreases by ca. 40%, the low-mass dilepton enhancement over the cocktail indicates an increase over the result at 158 AGeV, consistent with the anticipated prevalence of baryon-driven medium effects. The predictions from the in-medium broadened ρ spectral function describe the data well. This trend continues all the way down to relativistic energies in the BEVALAC/SIS regime ($E_{\text{lab}}=1-2$ AGeV), where a large excess radiation has also been reported [41, 42]. The next step is to go to higher energies as available at the colliders RHIC and LHC. Here, the net baryon density at mid-rapidity becomes small. It was pointed out, however, that at temperatures close to T_{pc} , the *sum* of the densities of baryons (B) and anti-baryons (\bar{B}) is appreciable, about $0.7\rho_0$, and thus critical in producing a large broadening of the ρ , since it interacts equally with baryons and anti-baryons due to CP invariance [43]. Since the concept of chemical freeze-out continues to hold in nuclear collisions at RHIC energy, the total number of baryons plus anti-baryons does not change appreciably until thermal freeze-out at $T_{fo}\simeq 100$ MeV, and thus their density drops much slower than would be the case in chemical equilibrium (where it would decrease dramatically due to the large mass penalty on baryons). The upshot of this discussion is that the hadronic in-medium effects at collider energies were predicted to be comparable to that at SPS energies, and thus the low-mass dilepton enhancement at RHIC and LHC is expected to be quite similar in magnitude and shape to what has been observed at SPS. The PHENIX data of Ref. [44] do not support this expectation: a large enhancement in central Au-Au($\sqrt{s}=200$ AGeV) has been reported which cannot be described by the in-medium hadronic effects as is the case at the SPS. One should note, however, that the enhancement in non-central collisions is significantly smaller. A new mechanism should thus be operative in central Au-Au at RHIC, which does not prominently figure at SPS, nor in more peripheral collisions at RHIC. On the other hand, the STAR collaboration has reported preliminary data for dielectrons in central Au-Au($\sqrt{s}=200$ AGeV) [45], which indicate a much smaller enhancement, not incompatible with the effects expected from the in-medium ρ broadening. At the recent Quark Matter 2012 meeting, the STAR collaboration went another step further, presenting a systematic dielectron measurement from the RHIC beam-energy scan program [46]. A persistent low-mass enhancement was found in Au-Au at collision energies of $\sqrt{s}=19.6, 39, 62$ and 200 AGeV. The invariant-mass spectra at the lowest energy (19.6 GeV) exhibited the largest excess over the cocktail, and agree very well with the CERES data in Pb-Au($\sqrt{s}=17.3$ AGeV). The predictions from hadronic many-body theory (with a moderate QGP portion in the low-mass regime) show good agreement with this excitation function. The STAR measurements (together with the CERES and NA60 data) thus suggest a universal origin of the low-mass dilepton enhancement in URHICs from $\sqrt{s}\simeq 10-200$ GeV. New data reported by the PHENIX collaboration for peripheral and semi-central Au-Au, taking advantage of the hadron blind detector (HBD), also support this scenario [47].

The STAR collaboration furthermore presented first measurements of the dielectron elliptic flow, v_2 . Within the currently rather large uncertainties of this very challenging measurement, the v_2 of the dielectrons in the low-mass region, divided up into several mass bins, was found to be compatible with the simulated v_2 of the decay cocktail (mostly due to the long-lived π , η , ω and ϕ contributions). At face value, this result implies that the excess radiation carries a v_2 which is as large as the hadrons decaying after thermal freezeout. This assertion is, in fact, very consistent with the PHENIX measurement of direct photon v_2 in Au-Au collisions [48], which was found to be compatible with those of pions for $q_T \leq 3$ GeV. Such an observation is difficult to account for through radiation which is dominated by early QGP emission [49, 50, 51]. This discrepancy can be noticeably reduced in a rather straightforward fireball scenario where most of the bulk v_2 is built up by the time the system reaches the phase transition region, in connection with photon emission rates for QGP and hadronic matter which continuously evolve across T_{pc} [52]. The latter feature is indeed satisfied when merging hadronic many-body calculations for photon production [37] with QGP rates in a complete leading-order perturbative evaluation [53]. At the same time, a fireball evolution with fully built-up elliptic flow and fairly large radial flow at $\sim T_{pc}$, is supported empirically by the systematics of the measured spectra and v_2 of multistrange particles (Ω^- , ϕ and Ξ), as well as by the constituent quark-number scaling of light and strange hadrons; it is possible to realize these features in explicit hydrodynamic simulations [54]. Furthermore, the PHENIX collaboration extracted an inverse slope of their excess direct-photon spectra (defined by subtracting the primordial contribution from hard NN collisions; late decays, such as $\pi^0, \eta \rightarrow \gamma\gamma$, are already taken out in the definition of “direct” photons). It was found to be $T_{\text{eff}} \simeq (221 \pm 19^{\text{stat}} \pm 19^{\text{sys}})$ MeV. This is a rather soft slope given its approximate decomposition into a true medium temperature and the blue-shift effect on massless particles due to an average radial flow velocity, $T_{\text{eff}} \simeq T\sqrt{(1 + \beta_{\text{av}})/(1 - \beta_{\text{av}})}$. For example, for an average flow velocity of $\beta_{\text{av}} = 0.3(0.4)$, the blue-shift correction amounts to $\sim 35(50)\%$. This further corroborates that the prevalent emission of the photons measured by PHENIX should be around T_{pc} .

To summarize this section, the excess of EM radiation observed in URHICs to date is remarkably consistent with a thermal source of dileptons and photons from a hydrodynamically evolving medium, and thus naturally fits into the current “standard model” of these reactions. Employing state-of-the-art emission rates allows for an accurate description of precision dilepton data at the SPS, and accounts for data available at both lower SPS energy and the most the recent spectra obtained in a first systematic energy scan in the collider regime of RHIC. Slope analyses of both mass and q_T spectra, as well as their large v_2 , give strong indications for this excess radiation to emanate from around the phase transition temperature predicted by thermal lattice QCD. The similarity in magnitude and spectral shape of the excess radiation over the now available formidable range in collision energy suggests a universal origin of the observations (and further points to emission around T_{pc}). In the following section we will revisit how microscopic mechanisms of in-medium ρ broadening, which is consistent with the data, relates to chiral symmetry restoration in the medium.

3. Implications for Chiral Restoration

Rigorous connections between chiral order parameters and the ρ spectral function (or more precisely: vector-isovector spectral function) can be made via well-known sum rule techniques. These are usually divided into two classes, namely the QCD sum rules (QCDSRs) [55] and Weinberg (or chiral) sum rules (WSRs) [56, 57]. The former are formulated in a given hadronic channel and utilize a dispersion integral to relate the physical spectral function to an expansion in spacelike momentum transfer with coefficients governed by quark and gluon condensates

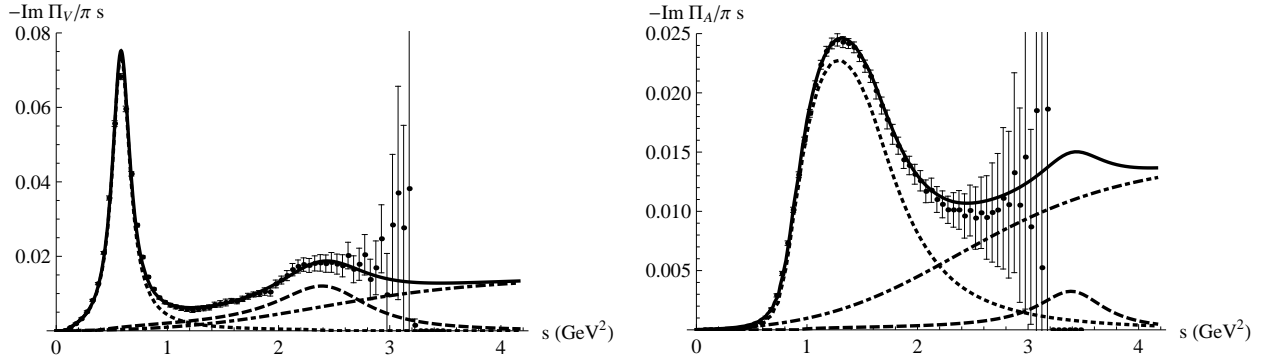


Figure 3. Vector (left panel) and axialvector (right panel) spectral functions in vacuum [61]. Notable features are the inclusion of excited states ρ' and a_1' (long-dashed lines) and a universal perturbative continuum (dash-dotted lines) which starts at significantly higher energies than in most previous sum-rule analyses.

(operator-product expansion). For the vector channel, one has

$$\frac{1}{M^2} \int_0^\infty ds \frac{\rho_V(s)}{s} e^{-s/M^2} = \frac{1}{8\pi^2} \left(1 + \frac{\alpha_s}{\pi} \right) + \frac{m_q \langle \bar{q}q \rangle}{M^4} + \frac{1}{24M^4} \left\langle \frac{\alpha_s}{\pi} G_{\mu\nu}^2 \right\rangle - \frac{56\pi\alpha_s}{81M^6} \langle \mathcal{O}_4^V \rangle \dots, \quad (4)$$

where $\rho_V = -\text{Im}\Pi_V/\pi$ is the spectral function, $\langle \bar{q}q \rangle$ the chiral condensate, $\langle \frac{\alpha_s}{\pi} G_{\mu\nu}^2 \rangle$ the gluon condensate and $\langle \mathcal{O}_4^V \rangle$ the vector 4-quark condensate. The WSRs are, in a sense, more closely related to chiral symmetry (breaking). They involve energy-weighted integrals (or moments) over the difference of vector and axialvector spectral functions, which directly result in order parameter of chiral symmetry breaking, such as the quark condensate, pion decay constant or chirally-breaking part of the 4-quark condensate. They read

$$f_n = \int_0^\infty ds s^n [\rho_V(s) - \rho_A(s)], \quad (5)$$

$$f_{-2} = f_\pi^2 \frac{\langle r_\pi^2 \rangle}{3} - F_A, \quad f_{-1} = f_\pi^2, \quad f_0 = f_\pi^2 m_\pi^2, \quad f_1 = -2\pi\alpha_s \langle \mathcal{O}_4^X \rangle \quad (6)$$

(r_π : pion charge radius, F_A : coupling constant for the radiative pion decay, $\pi^\pm \rightarrow \mu^\pm \nu_\mu \gamma$, $\langle \mathcal{O}_4^X \rangle$: chirally breaking 4-quark condensate), and are referred to as WSR-0 through -3. They have been shown to remain valid in the medium [58]. This is quite a fortunate situation as the in-medium vector spectral function is the only one readily available from experiment.

A quantitative use of these sum rules in medium requires to first establish their accuracy and sensitivity in vacuum. This has recently been revisited by simultaneously analyzing both sum-rule types in connection with τ -decay data [59, 60] which give accurate information on the vector and axialvector spectral function in vacuum up to energies of the τ mass, $\sqrt{s} < m_\tau \simeq 1.78$ GeV. The low-energy part of the vector spectral function has been taken from the microscopic model for the ρ meson that figures in the discussion of the dilepton data of the previous section, while the a_1 has been fit to the data with a Breit-Wigner ansatz. A novel element in this analysis is the postulate of a universal perturbative continuum in both vector and axialvector channel. Besides its underlying physical motivation of degeneracy in the perturbative domain, it also allows for an improved description of the intermediate-energy vector data through the introduction of a ρ' resonance. It then turns out that a quantitative agreement with the right-hand-side (*rhs*) of WSRs 0-2 unequivocally requires the presence of an excited axialvector resonance, at a mass of

about $m_{a_1} \simeq 1.8$ GeV (WSR-3 also shows a large improvement) [61]. This indicates a rather high sensitivity of the WSRs to chiral breaking effects. Another way of looking at this is to examine the values of the integrals on the *rhs* of the WSRs, Eq. (5), as a function of the upper integration limit, $I_n(s_{\text{up}})$. One finds oscillations with an amplitude much larger than the asymptotic values as given by the left-hand side (*lhs*), i.e., the latter are a result of formidable cancellations and therefore are to be considered as “small”. Finally, the thus constructed vacuum spectral functions have been tested with their respective QCDSR [61]. Within the current theoretical uncertainties of the additionally involved chiral blind operators, such as the gluon condensate, these are also reasonably well satisfied, within a typical margin of $\sim 0.5\%$.

Let us now turn to the evaluation of the sum rules in medium (see, e.g., Ref. [62] for a recent survey). As a first step, it is instructive to examine the consequences of model-independent low-temperature expansions. As shown in Ref. [63], the leading T -dependence in the vector and axial-vector channels in the chiral limit amounts to a mutual mixing of their vacuum form, $\Pi_{V,A}^0$, as

$$\Pi_{V,A}(q; T) = (1 - \varepsilon(T)) \Pi_{V,A}^0(q) + \varepsilon(T) \Pi_{A,V}^0(q), \quad (7)$$

with the mixing parameter $\varepsilon(T) = T^2/6f_\pi^2$ (which is proportional to the scalar pion density). The physical process realizing the mixing is a resonant interaction of the ρ -meson with pions into an a_1 , $\rho + \pi \rightarrow a_1$. It turns out that the chiral mixing straightforwardly satisfies the in-medium WSR-1 and -2, provided they are fulfilled in vacuum [58]. Complications can arise, however, at the level of the spectral functions, especially in set-ups with a rather small vector continuum threshold, where the latter does not separate from the nonperturbative resonance region of the axialvector, i.e., the a_1 mass. This problem does not occur in the implementations of degenerate continua with higher threshold energy [64, 61]; here, the continua stay invariant and the mixing only operates on the nonperturbative part of both spectral functions. One can furthermore evaluate the QCD sum rules in the mixing scenario [65, 66]). Employing the model-independent T -dependencies of quark and gluon condensates, one finds both vector and axialvector QCDSRs to be satisfied within 0.7% or so up to temperatures of $T=150$ MeV [65], where $\varepsilon \simeq 0.2$ so that the expansion starts to become unreliable (note that $\varepsilon \simeq 0.5$, which is reached at $T \simeq 225$ MeV (160 MeV in the chiral limit), corresponds to full mixing, i.e., degeneracy of V and A correlators in Eq. (7); thermal excitations other than the pion are expected to take over well before that). We recall that a mixing scenario can also be formulated in cold nuclear matter, through a coupling to the nuclear pion cloud [67, 68]. The coupling of these pions proceeds through the pion cloud of the ρ , thereby creating axial currents [68].

While conceptually attractive (and rigorous), the V - A mixing mechanism alone is insufficient to account for medium effects necessary to understand dilepton data. Most importantly, it lacks the broadening of the ρ spectral shape that is pivotal in the description of the low-mass excess observed in experiment. We recall that this broadening is essentially due to two mechanisms [24]: one is the medium modification of the ρ -meson’s pion cloud (which includes virtual pion-exchange processes, i.e., chiral mixing), and the other is due to direct resonance interactions of the ρ with heat bath particles h , $\rho + h \rightarrow R$, leading to the excitation of further resonances, R . How are these processes related to chiral symmetry restoration? To elaborate on this question, let us recall the model-independent, low-temperature and low-density result for the chiral condensate in a dilute hadronic medium (e.g., pion or nucleon gas) which reads [69, 70, 71]

$$\frac{\langle \bar{q}q \rangle(T, \mu_B)}{\langle \bar{q}q \rangle_0} = 1 - \sum_h \frac{\varrho_h^s \Sigma_h}{m_\pi^2 f_\pi^2} \simeq 1 - \frac{T^2}{8f_\pi^2} - \frac{1}{3} \frac{\varrho_N}{\varrho_0} - \dots \quad (8)$$

with ϱ_h^s : scalar density of hadron h . The sigma term, $\Sigma_h = m_q \langle h | \bar{q}q | h \rangle$, can be defined as the expectation value of the chiral-symmetry breaking term of the QCD Lagrangian inside a hadron h . For the pion and nucleon they have been evaluated from both chiral perturbation

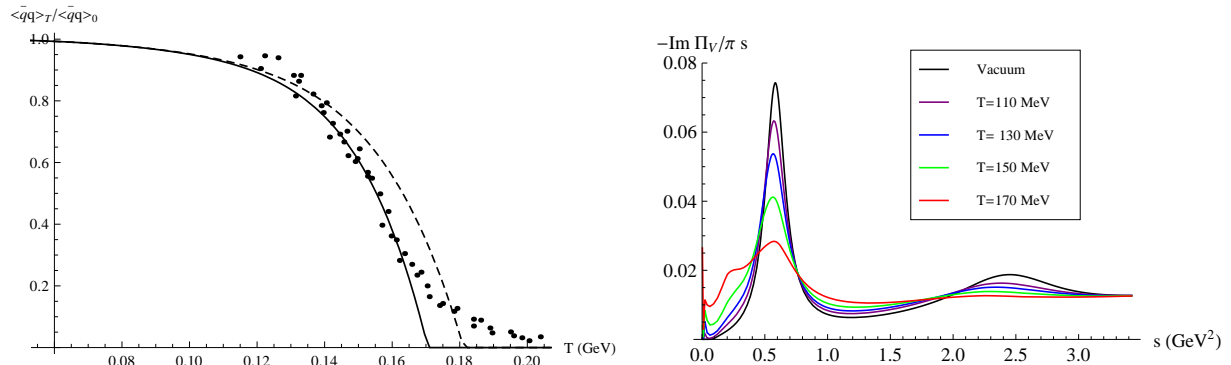


Figure 4. Left panel: Temperature dependence of the chiral quark condensate, normalized to its vacuum value, as obtained from thermal lattice QCD [78] for different temporal lattice sizes (indicated by different symbols); the dashed line is the hadron-resonance gas result where the condensate is diminished by the quark content of the thermal excitations; the solid line includes a T^{10} correction which improves the agreement with lattice data at $T > 140$ MeV. Right panel: In-medium vector spectral functions in the isovector channel including the calculated in-medium ρ contributions at vanishing chemical potential at low mass [24], supplemented with an in-medium ρ' contribution and a fixed perturbative continuum as deduced from in-medium QCD sum rules [76].

theory [69, 70, 71] and lattice QCD [72]. The second equality in Eq. (8) follows from the chiral limit for the pion and a value of $\Sigma_N=45$ MeV for the nucleon. More recent evaluations suggest the latter to be significantly larger, around 60 MeV [72]. The above expression has been generalized to a resonance gas of hadrons to leading order in their densities. Note that, although there are formally no interactions included, the excited hadronic states may be thought of as being built up by resonance interactions of the stable pions and nucleons. In the nonrelativistic limit, the pertinent sigma terms may be estimated using $\bar{q}q \simeq q^\dagger q$, so that Σ_h/m_q simply counts the number of light quarks in h . With $\Sigma_h > 0$, one obtains the well-known result that the mere presence of hadrons diminishes the (negative) chiral condensate of the vacuum, $\langle 0|\bar{q}q|0\rangle \equiv \langle \bar{q}q \rangle_0 \simeq -2 \text{ fm}^{-3}$ per light-quark flavor, i.e., the “vacuum cleaner” effect. The very existence of the resonance excitations in the hadron gas, which is one of the components in the ρ -meson broadening, is thus intimately related to the reduction of the chiral condensate. This notion can be carried further by realizing that the sigma term can be decomposed into a short-distance part associated with the hadron’s quark core and a long-distance part associated with its pion cloud, $\Sigma_h = \Sigma_h^{\text{core}} + \Sigma_h^\pi$, see, e.g., Refs. [73, 74] for the nucleon case. These two terms naturally find their counterparts in the medium effects of the ρ spectral function, namely the ones induced by direct resonance excitations as well as through the coupling of its pion cloud to the medium, respectively. This puts the medium effects due to chiral mixing through (virtual) pions and due to the hadron-resonance gas excitations on equal footing. Also recall that the hadron-resonance gas appears to be a good approximation to the QCD partition function for temperatures up to close to (and even slightly above) T_{pc} [75].

The next question is how this connection works out more quantitatively when analyzing the in-medium sum rules. This has been revisited very recently [76] (see also Ref. [77]), by adopting the newly suggested description of the vector correlator with ground and excited state and a universal high-energy continuum (recall Fig. 3). For the ground state the in-medium ρ spectral function as used in dilepton calculations has been employed, while the perturbative continuum remains unchanged. This leaves the Breit-Wigner parameters of the in-medium ρ' to be adjusted (in lieu of the continuum threshold in previous QCDSR analyses). For

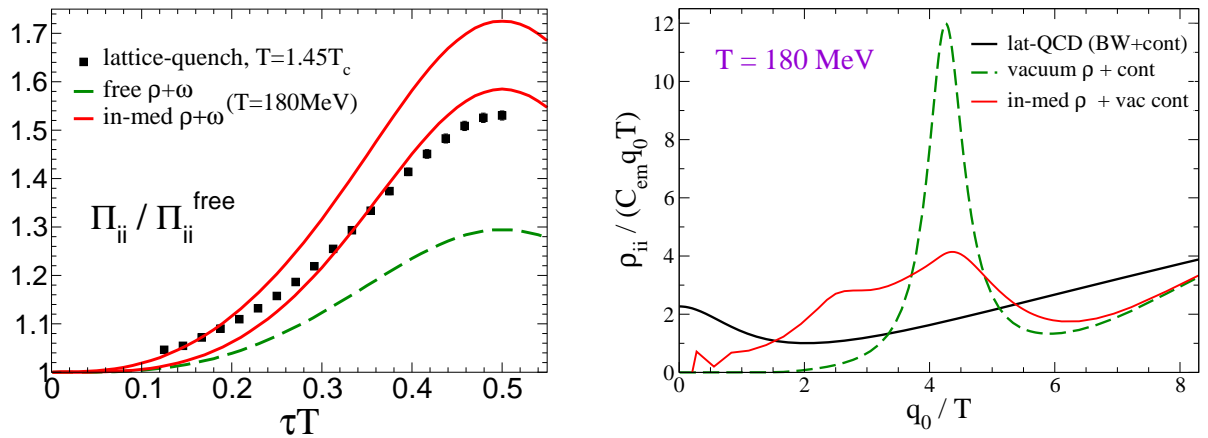


Figure 5. Left panel: Euclidean correlators at vanishing 3-momentum and normalized to the free $q\bar{q}$ continuum (for $N_f=2$ light quarks), as a function of imaginary time, τ , in units of inverse temperature; the thermal lattice QCD results in quenched approximation at $1.45 T_c$ (black squares) [79] are compared to effective hadronic model evaluations of Eq. (9) [80] using either vacuum ρ and ω spectral functions plus continuum (dashed line), or in-medium ρ and ω [24] at $T=180$ MeV with either vacuum or in-medium reduced continuum (lower and upper solid line, respectively). Right panel: Spectral functions (normalized by isospin degeneracy, temperature and energy) corresponding to the correlators in the left panel; the IQCD result (black solid line) is extracted from the data points in the right panel by a 3-parameter fit ansatz [79]; for the hadronic spectral functions only the isovector part is shown (ρ meson plus continuum), where the in-medium one (red line) uses a vacuum continuum and thus corresponds to the lower red line in the left panel.

the temperature dependence of the condensates, the “non-interacting” hadron-resonance gas expression, Eq. (8), has been used for the 2-quark condensate, which turns out to agree rather well with lattice data, cf. left panel of Fig. 4 (a small correction has been introduced to better reproduce the lattice data in the vicinity of T_{pc}^X). The 4-quark and gluon condensate are treated analogously, where the former includes correction terms to vanish at the same temperature as the 2-quark condensate. It turns out that the QCDSRs can be rather well satisfied even until close to the vanishing of the quark condensates, provided that the ρ' also melts, cf. right panel of Fig. 4. Of course, one should keep in mind that the vanishing of the quark condensates in the hadron-resonance gas is unrelated to a real phase transition, although it may still indicate that this model captures basic aspects of the medium when extrapolated close to T_{pc} . This argument also applies to the in-medium calculations of the ρ spectral function which should be rather reliable up to temperatures of about $T \simeq 150$ MeV, where the total hadron density has reached about $2\varrho_0$. As discussed in the previous section, it is quite intriguing that dilepton data support a smooth extrapolation of the medium effects into the transition region. The analyses of the WSRs in this framework requires the knowledge of the in-medium axialvector spectral function, which is not available (yet). Preliminary studies using ansätze for the in-medium Breit-Wigner shape for a_1 and a_1' that satisfy the axialvector QCDSR, indicate agreement with the in-medium WSRs, with a tendency of the vector and axialvector to degenerate into rather structureless spectral functions.

Another test of the in-medium vector spectral function, and of the associated chiral-restoration mechanism, can be provided by thermal lattice QCD. In the latter, the information on the correlation function in a specific hadronic channel, α , is routinely computed in euclidean

time, $\Pi_\alpha(\tau, \vec{r})$. After a Fourier transform in the spatial coordinates (from \vec{r} to \vec{q}), the relation to the spectral function in the physical (timelike) regime takes the form

$$\Pi_\alpha(\tau, q; T) = \int_0^\infty \frac{dq_0}{2\pi} \rho_\alpha(q_0, q; T) \frac{\cosh[q_0(\tau - 1/2T)]}{\sinh[q_0/2T]}. \quad (9)$$

Thus, via simple a integration over a model spectral function one can directly compare to “lattice data”. The computational effort to compute the euclidean correlators in full QCD with dynamical quarks is formidable and no results for light vector mesons are currently available. However, in the quenched approximation, these calculations have achieved good accuracy in a gluon plasma above T_c [79]. It is instructive to compare the trends in these computations to what one obtains from the spectral functions used in the interpretation of dilepton data. This is shown in the left panel of Fig. 5, depicting the euclidean correlators normalized to the perturbative (non-interacting) $q\bar{q}$ continuum. The hadronic spectral function, extrapolated to a temperature of $T=180$ MeV, shows a significant enhancement at large τ which is a direct manifestation of the low-mass enhancement generated by medium effects (critical for the description of dilepton data). In fact, even the vacuum spectral function shows this effect, caused by the free ρ and ω resonances; the in-medium broadening roughly doubles this enhancement. The quenched lattice data [79] show a surprisingly similar trend, given that they are computed at $1.45 T_c$. Note that chiral symmetry is restored under these conditions [81]. To extract the spectral function from the lattice data is more involved. In Ref. [79] a physically motivated 3-parameter ansatz has been fit to the correlators resulting in a conductivity maximum at low-energy, followed by a smooth transition into the perturbative continuum at high energy (see black solid line in the right panel of Fig. 5). Comparing this to the hadronic spectral functions, one observes a trend suggestive of approaching the lattice data via a melting of the vacuum ρ resonance structure.

4. Conclusions

Low-mass dilepton data in ultrarelativistic heavy-ion collisions provide a unique glimpse at the vector spectral function inside the produced hot and dense medium. After the initial discovery of large medium effects in the early and mid 90’s, recent data are now allowing for quantitative tests of theoretical calculations. At SPS energies, a strongly broadened ρ -meson spectral function, due to many-body effects in hot and dense hadronic matter, accounts well for both CERES and NA60 data. Slope analyses of invariant-mass and transverse-momentum spectra corroborate that the observed spectral modifications at low mass originate from temperatures in the vicinity of the QCD transition region, $T_{pc} \simeq 160$ -170 MeV. If this picture is correct, very similar effects are expected for the low-mass dilepton spectra at collider energies. Very recent STAR data have given first evidence for the universality of the low-mass excess with collision energy, but are hopefully only the beginning of a systematic multi-differential investigation of dilepton observables. The transition from the baryon-rich to net-baryon free matter is a critical test of the current understanding of medium effects driven by baryon plus anti-baryon densities in the vector spectral function. At the same time, the large PHENIX photon- v_2 is most naturally associated with radiation from around T_{pc} , even at full RHIC energy. The large PHENIX dilepton excess in central Au-Au remains a puzzle which most likely requires a new type of radiation source.

We have then argued that the mechanisms underlying these medium effects, namely resonance excitations and (virtual) pion-cloud modifications, find their direct counterpart in the sigma-terms of the heat-bath particles. This is significant as the sigma-terms are at the origin of the reduction of the chiral quark condensate. Even though this mechanism only captures the leading dependence in the scalar density of the medium particles, it is remarkable that this ansatz describes the lattice data for the quark condensate rather well until close to the

(pseudo-) transition temperature. Although the resonance gas does not incorporate criticality, the resonance excitations represent interaction contributions which amount to higher orders in the density of the stable pions and nucleons. When evaluating the relation between the in-medium vector spectral function and the decreasing condensate(s) more quantitatively using QCD sum rules, a reasonable consistency is found; studies of the Weinberg sum rules are ongoing. Finally, the calculations of euclidean correlators and their comparison to current lattice data also reveal a common trend toward a rather structureless spectral function. All this suggests that the ρ -meson melting scenario is quite consistent with different angles on chiral symmetry restoration. To develop these indications into a quantitative proof, and/or unravel hitherto unknown aspects of chiral restoration, remains a challenge. Experimental information from the collider experiments will be critical in guiding further theoretical efforts, and vice versa.

Acknowledgment I thank H. van Hees, C. Gale and J. Wambach for fruitful collaboration, and P. Hohler and N. Holt for their recent contributions to the sum rule analyses. This work is supported by the US National Science Foundation under grant no. PHY-0969394 and by the A.-v.-Humboldt foundation.

References

- [1] R. Rapp, J. Wambach and H. van Hees, in *Relativistic Heavy-Ion Physics*, edited by R. Stock and Landolt Börnstein (Springer), New Series **I/23A** (2010) 4-1 [arXiv:0901.3289[hep-ph]].
- [2] I. Tserruya, in *Relativistic Heavy-Ion Physics*, edited by R. Stock and Landolt Börnstein (Springer), New Series **I/23A** (2010) 4-2 [arXiv:0903.0415[nucl-ex]].
- [3] H.J. Specht [for the NA60 Collaboration], AIP Conf. Proc. **1322**, 1 (2010).
- [4] R. Rapp, Acta Phys. Polon. B **42**, 2823 (2011).
- [5] C. Gale, arXiv:1208.2289 [hep-ph].
- [6] G. Agakichiev *et al.* [CERES Collaboration], Phys. Rev. Lett. **75**, 1272 (1995).
- [7] G. Agakichiev *et al.* [CERES Collaboration], *Eur. Phys. J. C* **41**, 475 (2005).
- [8] D. Adamova *et al.* [CERES/NA45 Collaboration], Phys. Lett. B **666**, 425 (2008).
- [9] G.-Q. Li, C.M. Ko and G.E. Brown, Phys. Rev. Lett. **75**, 4007 (1995).
- [10] G.E. Brown, M. Harada, J.W. Holt, M. Rho and C. Sasaki, Prog. Theor. Phys. **121**, 1209 (2009)
- [11] G. Chanfray and P. Schuck, Nucl. Phys. A **555**, 329 (1993).
- [12] M. Herrmann, B.L. Friman and W. Nörenberg, Nucl. Phys. A **560**, 411 (1993).
- [13] B. Friman and H.J. Pirner, Nucl. Phys. A **617**, 496 (1997).
- [14] F. Klingl, N. Kaiser and W. Weise, Nucl. Phys. A **624**, 527 (1997).
- [15] W. Peters, M. Post, H. Lenske, S. Leupold and U. Mosel, Nucl. Phys. A **632**, 109 (1998).
- [16] M. Urban, M. Buballa, R. Rapp and J. Wambach, Nucl. Phys. A **641**, 433 (1998).
- [17] D. Cabrera, E. Oset and M. J. Vicente Vacas, Nucl. Phys. A **705**, 90 (2002).
- [18] K. Haglin, Nucl. Phys. A **584**, 719 (1995).
- [19] R. D. Pisarski, Phys. Rev. D **52**, 3773 (1995).
- [20] C. Song and V. Koch, Phys. Rev. C **54**, 3218 (1996).
- [21] R. Rapp and C. Gale, Phys. Rev. C **60**, 024903 (1999).
- [22] A. Ayala and J. Magnin, Phys. Rev. C **68**, 014902 (2003)
- [23] R. Rapp, G. Chanfray and J. Wambach, Phys. Rev. Lett. **76**, 368 (1996).
- [24] R. Rapp and J. Wambach, *Eur. Phys. J. A* **6**, 415 (1999).
- [25] V.L. Eletsky, M. Belkacem, P.J. Ellis and J.I. Kapusta, Phys. Rev. C **64**, 035202 (2001).
- [26] S. Ghosh and S. Sarkar, Nucl. Phys. A **870-871**, 94 (2011) [Erratum-ibid. A **888**, 44 (2012)].
- [27] R. Arnaldi *et al.* [NA60 Collaboration], *Eur. Phys. J. C* **61**, 711 (2009).
- [28] H. van Hees and R. Rapp, Nucl. Phys. A **806**, 339 (2008)
- [29] R. Arnaldi *et al.* [NA60 Collaboration], Phys. Rev. Lett. **96**, 162302 (2006).
- [30] H. van Hees and R. Rapp, Phys. Rev. Lett. **97**, 102301 (2006) [hep-ph/0603084].
- [31] K. Dusling, D. Teaney and I. Zahed, Phys. Rev. C **75**, 024908 (2007) [nucl-th/0604071].
- [32] J. Ruppert, C. Gale, T. Renk, P. Lichard and J. I. Kapusta, Phys. Rev. Lett. **100**, 162301 (2008)
- [33] E. Santini, J. Steinheimer, M. Bleicher and S. Schramm, Phys. Rev. C **84**, 014901 (2011)
- [34] O. Linnyk, E.L. Bratkovskaya, V. Ozvenchuk, W. Cassing and C.M. Ko, Phys. Rev. C **84**, 054917 (2011)
- [35] R. Rapp, Nucl. Phys. A **661**, 33 (1999).
- [36] J.I. Kapusta, P. Lichard and D. Seibert, Phys. Rev. D **44**, 2774 (1991) [Erratum-ibid. D **47**, 4171 (1993)].

- [37] S. Turbide, R. Rapp and C. Gale, Phys. Rev. C **69**, 014903 (2004).
- [38] R. Arnaldi *et al.* [NA60 Collaboration], Phys. Rev. Lett. **100**, 022302 (2008).
- [39] R. Rapp, M. Urban, M. Buballa, and J. Wambach, Phys. Lett. B **417**, 1 (1998).
- [40] D. Adamova *et al.* [CERES/NA45 Collaboration], Phys. Rev. Lett. **91**, 042301 (2003).
- [41] R.J. Porter *et al.* (DLS Collaboration), Phys. Rev. Lett. **79**, 1229 (1997).
- [42] G. Agakishiev *et al.* [HADES Collaboration], Phys. Rev. C **84**, 014902 (2011)
- [43] R. Rapp, Phys. Rev. C **63**, 054907 (2001).
- [44] A. Adare *et al.* [PHENIX Collaboration], Phys. Rev. C **81**, 034911 (2010).
- [45] J. Zhao [STAR Collaboration], J. Phys. G **38**, 124134 (2011).
- [46] F. Geurts *et al.* [STAR Collaboration], talk at Quark Mater 2012 International Conference (Washington, DC), Aug. 13-18, 2012.
- [47] I. Tserruya *et al.* [PHENIX Collaboration], talk at Quark Mater 2012 International Conference (Washington, DC), Aug. 13-18, 2012.
- [48] A. Adare *et al.* [PHENIX Collaboration], arXiv:1105.4126 [nucl-ex].
- [49] F. -M. Liu, T. Hirano, K. Werner and Y. Zhu, Phys. Rev. C **80**, 034905 (2009).
- [50] H. Holopainen, S. Rasanen and K. J. Eskola, Collider,” Phys. Rev. C **84**, 064903 (2011).
- [51] M. Dion, J. -F. Paquet, B. Schenke, C. Young, S. Jeon and C. Gale, Phys. Rev. C **84**, 064901 (2011).
- [52] H. van Hees, C. Gale and R. Rapp, Phys. Rev. C **84**, 054906 (2011).
- [53] P.B. Arnold, G.D. Moore and L.G. Yaffe, JHEP **0112**, 009 (2001).
- [54] M. He, R.J. Fries and R. Rapp, Phys. Rev. C **85**, 044911 (2012).
- [55] M.A. Shifman, A.I. Vainshtein, and V.I. Zakharov, Nucl. Phys. B **147**, 385 (1979).
- [56] S. Weinberg, Phys. Rev. Lett. **18**, 507 (1967).
- [57] T. Das, V. S. Mathur, and S. Okubo, Phys. Rev. Lett. **19**, 859 (1967).
- [58] J.I. Kapusta and E.V. Shuryak, Phys. Rev. D **49**, 4694 (1994).
- [59] R. Barate *et al.* (ALEPH Collaboration), Eur. Phys. J. C **4**, 409 (1998).
- [60] K. Ackerstaff *et al.* (OPAL Collaboration), Eur. Phys. J. C **7**, 571 (1999).
- [61] P.M. Hohler and R. Rapp, Nucl. Phys. A **892**, 58 (2012).
- [62] B. Friman, (ed.), C. Hohne, (ed.), J. Knoll, (ed.), S. Leupold, (ed.), J. Randrup, (ed.), R. Rapp, (ed.) and P. Senger, (ed.), Lect. Notes Phys. **814**, 1 (2011).
- [63] M. Dey, V. L. Eletsky, and B. L. Ioffe, Phys. Lett. B **252**, 620 (1990).
- [64] E. Marco, R. Hofmann and W. Weise, Phys. Lett. B **530**, 88 (2002).
- [65] N. Holt, P.M. Hohler and R. Rapp, in preparation (2012).
- [66] Y. Kwon, C. Sasaki and W. Weise, Phys. Rev. C **81**, 065203 (2010).
- [67] B. Krippa, Phys. Lett. B **427**, 13 (1998).
- [68] G. Chanfray, J. Delorme, M. Ericson and M. Rosa-Clot, Phys. Lett. B **455**, 39 (1999).
- [69] P. Gerber and H. Leutwyler, Nucl. Phys. B **321**, 387 (1989).
- [70] E. G. Drukarev and E. M. Levin, Prog. Part. Nucl. Phys. **27**, 77 (1991).
- [71] T. D. Cohen, R. J. Furnstahl, and D. K. Griegel, Phys. Rev. C **45**, 1881 (1992).
- [72] J. Martin Camalich, L. S. Geng and M. J. Vicente Vacas, Phys. Rev. D **82**, 074504 (2010).
- [73] I. Jameson, A.W. Thomas and G. Chanfray, J. Phys. G **18**, L159 (1992).
- [74] M.C. Birse and J.A. McGovern, Phys. Lett. **B292**, 242 (1992).
- [75] F. Karsch, K. Redlich and A. Tawfik, Eur. Phys. J. C **29**, 549 (2003).
- [76] P.M. Hohler and R. Rapp, arXiv:1209.1051 [hep-ph].
- [77] A. Ayala, C. A. Dominguez, M. Loewe and Y. Zhang, arXiv:1210.2588 [hep-ph].
- [78] S. Borsanyi, Z. Fodor, C. Hoelbling, S.D. Katz, S. Krieg, C. Ratti and K.K. Szabo [Wuppertal-Budapest Collaboration], JHEP **1009**, 073 (2010).
- [79] H.T. Ding, A. Francis, O. Kaczmarek, F. Karsch, E. Laermann and W. Soeldner, Phys. Rev. D **83**, 034504 (2011).
- [80] R. Rapp, Eur. Phys. J. A **18**, 459 (2003).
- [81] G. Boyd, S. Gupta, F. Karsch, E. Laermann, B. Petersson and K. Redlich, Phys. Lett. B **349**, 170 (1995).